The crystal structure, magnetism, and colossal magnetoresistance of Y_2CrS_4*

Liu Rong-Deng(刘荣灯)[a)b)], Liu Yun-Tao(刘蕴韬)[a)], He Lun-Hua(何伦华)[b)], Wang Zhi-Cui(王志翠)[b)], Chen Dong-Feng(陈东风)[a)], and Wang Fang-Wei(王芳卫)[b)†]

[a)] *China Institute of Atomic Energy, Beijing* 102413, *China*

[b)] *State Key Laboratory of Magnetism, Beijing National Laboratory for Condensed Matter Physics, Institute of Physics, Chinese Academy of Sciences, Beijing* 100190, *China*

(Received 5 January 2012; revised manuscript received 18 January 2012)

Ternary yttrium chromium sulfide, Y_2CrS_4, prepared by the solid-state reaction of Y_2S_3, Cr, and S, was found to exhibit an antiferromagnetic transition at about 64 K. The X-ray diffraction pattern at 300 K was refined with space group $Pca2_1$, and the structure parameters were determined to be $a = 12.51$ Å, $b = 7.53$ Å, and $c = 12.49$ Å. We investigated the magnetotransport properties, and observed negative colossal magnetoresistance reaching up to 2.5×10^4% in the semiconducting compound of Y_2CrS_4.

Keywords: magnetoresistance, crystal structure, magnetism

PACS: 75.47.Gk, 61.50.–f, 75.60.Ej **DOI:** 10.1088/1674-1056/21/5/057501

1. Introduction

In recent years, interest in colossal magnetoresistance (CMR) materials has grown, not only for fundamental scientific research but also practical applications in material engineering.[1−6] So far, three classes of CMR materials have been found.[7] They are (i) manganese oxides derived from $LaMnO_3$, which have a perovskite structure and exhibit the CMR effect in the vicinity of the magnetic transition temperature; (ii) compounds with the general formula of AB_2X_4, where A and B are transition-metal cations occupying the tetrahedral and octahedral sites, respectively, and X is a chalcogen, including Cr-based chalcogenide spinels[1] such as $HgCr_2S_4$;[8] (iii) pyrochlore oxides with a space group of Fd-3m and a composition of $A_2B_2O_7$ crystallized in the face-centred-cubic structure with eight formula units per unit cell, where A is a larger cation and B is a smaller transition metal cation. The most typical example is $Tl_2Mn_2O_7$.[9] In the three systems, units of slightly distorted $(Mn/Cr)O_6$ octahedra with or without Jahn–Teller ions are always found.

The CrS_6 octahedra are found in ternary yttrium chromium sulfide Y_2CrS_4, which has an orthorhombic structure and belongs to space group $Pca2_1$ (No. 29).[10] As the divalent chromium ions are Jahn–Teller ions with d^4 configuration, the CrS_6 octahedra in the structure are slightly distorted by the Jahn–Teller effect. It is difficult to grow Y_2CrS_4, so the electronic properties have not been investigated. In this paper, we report on the crystal structure, the magnetic properties, and the magnetotransport properties of Y_2CrS_4.

2. Experiments

The polycrystalline sample of Y_2CrS_4 was prepared by the standard solid-state synthesis method. High-purity powders of yttrium sulfide (Y_2S_3), chromium (Cr), and sulphur (S) were mixed homogeneously in proportions corresponding to the chemical formula, and then pelletized and sealed in an evacuated quartz tube. The tube was heated at 1275°C for 50 h.

The phase composition and structure were checked by powder X-ray diffraction (XRD) using a RINT 2400 diffractometer from the Rigaku Corporation with graphite monochromatized Cu $K\alpha$ radiation at room temperature.

*Project supported by the National Basic Research Program of China (Grant No. 2010CB833102) and the National Natural Science Foundation of China (Grant No. 10974244).

†Corresponding author. E-mail: fwwang@aphy.iphy.ac.cn

© 2012 Chinese Physical Society and IOP Publishing Ltd

The direct-current (dc) magnetic susceptibilities were measured under an applied field of 0.05 T in a temperature range of 4–300 K by using a Squid magnetometer (Quantum Design, MPMSXL-7), and the magnetic hysteresis loop was measured at 4 K.

The dc resistivity was measured with the standard four-contact method using a physical property measurement system (PPMS, Quantum Design), and the electrical contacts were established by using silver paint on a bar-shaped sample.

3. Results and discussion

Figure 1(a) displays the XRD patterns of Y_2CrS_4 (including the experimental and Rietveld calculated results), which reveal that the structure of the sample has an orthorhombic unit cell and pertains to space group $Pca2_1$. The weight pattern factor and the expected factor from the Rietveld refinement are $R_{wp} = 15.7\%$ and $R_{exp} = 8.46\%$, respectively. The structures of crystal Er_2CrS_4[11,12] and the previous report[10] were used as the initial parameters for the Fullprof program,[13] respectively. All the atoms were at the 4a sites, and the isotropic atomic displacement parameters were fixed to be 0.3 Å^2. The refined results are shown in Table 1, and are similar to the results in the previous literature,[10,11] except for the atomic coordinates. The crystal structure of Y_2CrS_4 and the bond lengths between Cr and S calculated from the refined crystal structure of Y_2CrS_4 are presented in the insets of Fig. 1(a) and Fig. 1(b), respectively. The four bonds connecting to each Cr are shorter than the other two bonds, which indicates that the CrS_6 octahedra are distorted by the Jahn–Teller effect, as are those in Er_2CrS_4.[14]

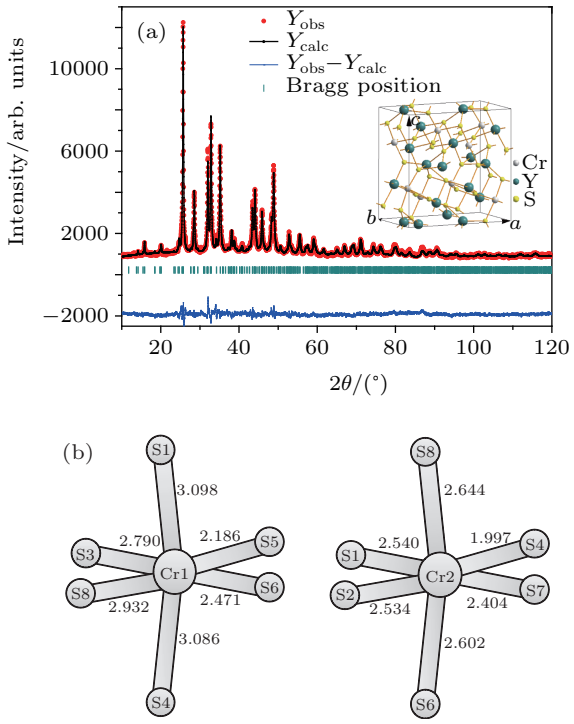


Fig. 1. (colour online) (a) Powder X-ray diffraction pattern fitted for Y_2CrS_4. The observed (dots) and calculated (line) patterns are shown on the top. The vertical marks in the middle show the positions calculated for the Bragg reflections. The lower trace is a plot of the difference between the calculated and observed intensities. The inset shows the crystal structure of Y_2CrS_4. (b) Distortions of the CrS_6 octahedra.

Table 1. Crystallographic data for Y_2CrS_4 at room temperature.

Space group			$Pca2_1$
a/Å			12.5068(1)
b/Å			7.5304(2)
c/Å			12.4905(4)
R_{wp}			15.7%
s			1.856
Atoms	x	y	z
Cr1	0.116(1)	0.628(2)	0.012(1)
Cr2	0.399(1)	0.104(3)	0.156(1)
Y1	0.1120(9)	0.112(2)	0.006(1)
Y2	0.1351(9)	0.373(2)	0.318(1)
Y3	0.382(1)	0.616(2)	0.150(1)
Y4	0.642(1)	0.138(2)	0.316(1)
S1	0.019(2)	0.123(4)	0.206(3)
S2	0.022(2)	0.629(5)	0.474(2)
S3	0.016(2)	0.683(4)	0.200(3)
S4	0.065(2)	0.138(5)	0.449(2)
S5	0.240(2)	0.350(6)	0.118(1)
S6	0.302(1)	0.615(5)	0.351(2)
S7	0.289(1)	0.107(6)	0.326(2)
S8	0.753(2)	0.144(7)	0.087(2)

The temperature dependences of the zero-field-cooled (ZFC) and field-cooled (FC) magnetic susceptibilities measured from 4 K to 300 K under an applied field of 0.05 T are shown in Fig. 2(a). An antiferromagnetic anomaly is found at about 64 K. The effective magnetic moment is deduced from the Curie–Weiss fitting of the linear part of the corresponding reciprocal magnetic susceptibility curve in the 150–300 K temperature range, $\mu_{eff} = 3.532\ \mu_B$. The value is between the theoretical effective magnetic moments of Cr^{2+} in the high spin state (4.90 μ_B) and low spin state (2.83 μ_B), and is close to the first-principles calculation results.[15] According to the LDA and the LDA+U calculations, the magnetic moments of Cr^{2+} at the antiferromagnetic phase are equal to 3.245 μ_B

and 3.739 μ_B, respectively. The neutron diffraction shows that the magnetic moment of Cr^{2+} is 3.27(9) μ_B at 10 K,[10] which is very close to our result. The Weiss constant is determined to be 13.78 K. The difference between ZFC and FC is observed below the Neel temperature. The shapes of the ZFC and FC curves below the Neel temperature indicate little ferromagnetic structure for Y_2CrS_4. Figure 2(b) displays a magnetic hysteresis loop measured at 4 K. A magnified view of the hysteresis loop at small fields (as illustrated in the inset of Fig. 2(b)) shows the remanent magnetization and the coercive force, which also indicate a simple ferromagnetic structure. Clearly, a nonlinear behavior is found within $H < 70$ kOe, indicating a complex magnetic structure.

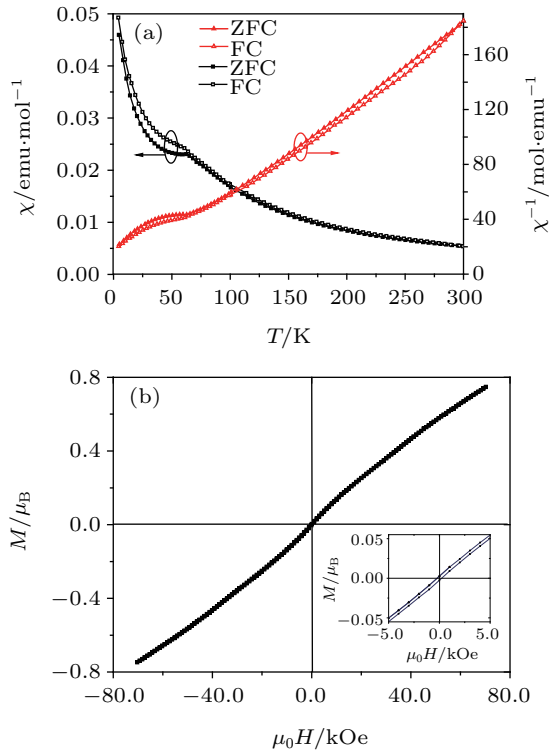


Fig. 2. (colour online) (a) Magnetic susceptibility and inverse magnetic susceptibility versus temperature measured at 0.05 T. (b) Magnetic hysteresis loop measured at 4 K; the inset gives a magnified view of the small fields.

In Fig. 3(a), the temperature dependences of the dc resistivity of Y_2CrS_4 measured using the four-point contact method with and without the applied field are shown. The dc resistivity exhibits a semiconducting behavior at low temperature (as illustrated in Fig. 3(b)) and is too large to be measured precisely at temperatures below 25 K. Under an external magnetic field of 10 T (current perpendicular to magnetic field geometry), the dc resistivity cannot be measured accurately at temperatures below 11 K. The dc resistivity varies strongly with the applied magnetic field. As illustrated in the inset of Fig. 3(a), the dc resistivity relative variation exceeds 250, and the CMR effect is up to the findings in most CMR manganites,[3,6,7,16–18,24] Cr-based chalcogenide spinels,[1,8,19,25,26] and pyrochlore oxides.[2,5,9,20–23] Y_2CrS_4 does not belong to the three classes of CMR compounds, as shown in Table 2. The former two classes of CMR compounds contain manganese and oxygen, and the latter two are composed of chromium and sulfur. The third class of CMR compounds includes trivalent chromium ions, while Y_2CrS_4 only has divalent Jahn–Teller chromium ions.

Table 2. The main characteristics of the four classes of CMR compounds.

	Class 1	Class 2	Class 3	Class 4
Example	$La_{0.67}Ba_{0.33}MnO_3$[24]	$Tl_2Mn_2O_7$[9,23]	$FeCr_2S_4$[25]	Y_2CrS_4
Octahedra	yes	yes	yes	yes
Jahn–Teller ions	yes	no	no	yes
Structure	perovskite	pyochlore	spinel	orthorhombic
Conductivity	insulator/conductor	conductor	semiconductor	semiconductor

Figure 3(b) shows the resistivity curves with and without the applied magnetic field replotted as $\ln\rho$–$1/T$ and $\ln(\rho/T)$–$1/T$, respectively. The Mott's variable-range hopping expression $\rho = \rho_0 \exp(T_0/T)^{1/4}$ cannot fit the curves (not shown here). The activation energy is deduced from the thermally activated behavior ($\rho = \rho_0 \exp(E/k_BT)$) due to a mobility edge fitting of the corresponding $\ln(\rho)$ curve in the 30–270 K reciprocal temperature range, $E_A = 33.6$ meV. Obviously, as shown in Fig. 3(b), the resistivity is due to the magnetic polaron hopping conduction, namely, $\rho = \rho_0 T \exp(E_P/k_BT)$, with $E_P = 39.96$ meV. The results are similar to those of $Fe_{1-x}Cd_xCr_2S_4$.[25,26] The reduction in spin-disorder scattering should be responsible for the CMR effect, which is probably enhanced at low charge carrier den-

sities. A detailed explanation requires an investigation using ultrafast mid-infrared spectroscopy.

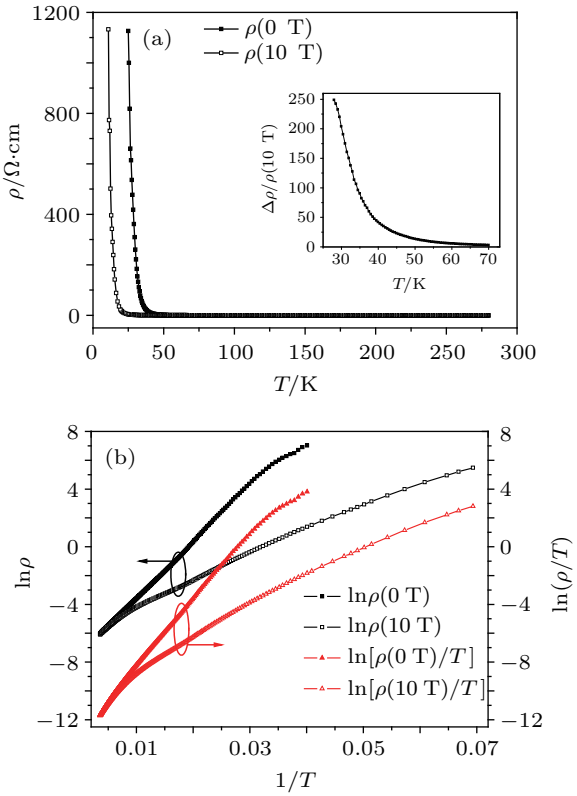


Fig. 3. (colour online) (a) The dc resistivities versus temperature measured at zero field and under an applied field of 10 T. The inset shows the magnetoresistance versus temperature for Y_2CrS_4, where $\Delta\rho/\rho(10\ \mathrm{T}) = [\rho(0\ \mathrm{T}) - \rho(10\ \mathrm{T})]/\rho(10\ \mathrm{T})$. (b) The dc resistivity curves with and without the applied magnetic field, replotted as $\ln\rho(H)$–$1/T$ and $\ln[\rho(H)/T]$–$1/T$.

4. Conclusion

In summary, we synthesized single-phase polycrystalline Y_2CrS_4 and refined the powder XRD pattern with the space group $Pca2_1$ by using the Fullprof program. The structure parameters obtained at 300 K were as follows: $a = 12.51$ Å, $b = 7.53$ Å, and $c = 12.49$ Å. The temperature dependences of the ZFC and FC magnetic susceptibilities were measured, and an antiferromagnetic anomaly was observed at about 64 K. A negative CMR in semiconducting Y_2CrS_4 was reported for the first time. The realization of CMR with an orthorhombic structure in compound Y_2CrS_4 should open up a vast range of materials for the further exploration and exploitation of this effect.

References

[1] Ramirez A P, Cava R J and Krajewski J 1997 *Nature* **386** 156

[2] Alonso J A, Velasco P, Martinez-Lope M J, Casais M T, Martinez J L, Fernandez-Diaz M T and de Paoli J M 2000 *Appl. Phys. Lett.* **76** 3274

[3] Salamon M B and Jaime M 2001 *Rev. Mod. Phys.* **73** 583

[4] Majumdar P and Littlewood P 1998 *Phys. Rev. Lett.* **81** 1314

[5] Prasankumar R P, Okamura H, Imai H, Shimakawa Y, Kubo Y, Trugman SA, Taylor A J and Averitt R D 2005 *Phys. Rev. Lett.* **95** 267404

[6] Millis A J, Shraiman B I and Mueller R 1996 *Phys. Rev. Lett.* **77** 175

[7] Ramirez A P 1997 *J. Phys.*: *Condens. Matter* **9** 8171

[8] Weber S, Lunkenheimer P, Fichtl R, Hemberger J, Tsurkan V and Loidl A 2006 *Phys. Rev. Lett.* **96** 157202

[9] Ramirez A P and Subramanian M A 1997 *Science* **277** 546

[10] Tezuka K, Shan Y J, Imoto H and Ohoyama K 2007 *J. Phys. Chem. Solids* **68** 2133

[11] Vaqueiro P, Szkoda I, Sanchez R D and Powell A V 2009 *Inorg. Chem.* **48** 1284

[12] Tomas A and Guittard M 1980 *Mater. Res. Bull.* **15** 1547

[13] Rodríguez-Carvajal J 2001 *FullProf* 2000 (Version July2001), Laboratoire Léon Brillouin (CEA-CNRS) France

[14] Tomas A, Chevalier R, Laruelle P and Bachet B 1976 *Acta Crystallogr.* B **32** 3287

[15] Wang B T, Yin W, Li W D and Wang F 2011 *Eur. Phys. J.* B **80** 307

[16] Wang J Y, Zhai W, Jin K X and Chen C L 2011 *Chin. Phys.* B **20** 097202

[17] Yang F, Jin K J, Huang Y H, He M, Lü H B and Yang G Z 2010 *Chin. Phys.* B **19** 087301

[18] Wang M and Zhang N 2006 *Chin. Phys.* **15** 850

[19] Sun C P, Huang C L, Lin C C, Her J L, Ho C J, Lin J Y, Berger H and Yang H D 2010 *Appl. Phys. Lett.* **96** 122109

[20] Alonso J A, Martinez J L, Martinez-Lope M J, Casais M T and Fernandez-Diaz M T 1999 *Phys. Rev. Lett.* **82** 189

[21] Cheong S W, Wang H Y, Batlogg B and Rupp L W 1996 *Solid State Commun.* **98** 163

[22] Velasco P, Alonso J A, Martinez-Lope M J, Casais M T and Martinez J L 2002 *J. Magn. Magn. Mater.* **242** 725

[23] Shimakawa Y, Kubo Y and Manako T 1996 *Nature* **379** 53

[24] von Helmolt R, Wecker J, Holzapfel B, Schultz L and Samwer K 1993 *Phys. Rev. Lett.* **71** 2331

[25] Yang Z R, Tan S, Chen Z W and Zhang Y H 2000 *Phys. Rev.* B **62** 13872

[26] Yang Z R, Bao X Y, Tan S and Zhang Y H 2004 *Phys. Rev.* B **69** 44407